Algal Research 52 (2020) 102099

Contents lists available at ScienceDirect

Algal Research

journal homepage: www.elsevier.com/locate/algal

Changes in lipid and carotenoid metabolism in *Chlamydomonas reinhardtii* during induction of CO_2-concentrating mechanism: Cellular response to low CO_2 stress☆

Ilka N. Abreu[a,h,1], Anna Aksmann[b,1], Amit K. Bajhaiya[c,j,*], Reyes Benlloch[d], Mario Giordano[e,f], Wojciech Pokora[b], Eva Selstam[g], Thomas Moritz[a,i,**]

[a] Umeå Plant Science Centre, Department of Forest Genetics and Plant Physiology, Swedish University of Agricultural Sciences, SE 90183 Umeå, Sweden
[b] University of Gdansk, Faculty of Biology, Department of Plant Physiology and Biotechnology, Wita Stwosza 59, 80-308 Gdansk, Poland
[c] Chemical Biological Centre (KBC), Department of Chemistry, Umeå University, SE 90187, Umeå, Sweden
[d] Departamento de Biología Vegetal, Facultad de Farmacia, Universidad de Valencia, 46100 Valencia, Spain
[e] Department of Life and Environmental Sciences, Universutà Politecnica delle Marche, Ancona, Italy
[f] STU-UNIVPM Joint Algal Research Center, Shantou, China
[g] Umeå Plant Science Centre, Department of Plant Physiology, Umeå University, SE 90187 Umeå, Sweden
[h] Department of Plant Biochemistry, University of Göttingen, Germany
[i] Novo Nordisk Foundation Center for Basic Metabolic Research, Faculty of Health and Medical Sciences, University of Copenhagen, Copenhagen DK-2200, Denmark
[j] Algal Biotechnology Lab, Department of Microbiology, School of Life Sciences, Central University of Tamil Nadu, Thiruvarur, Tamil Nadu 610005, India.

ARTICLE INFO

Keywords:
Betaine lipids
Carotenogenesis
CCM
Chlamydomonas
Lipid droplets
Low-CO_2 stress

ABSTRACT

Photosynthetic organisms strictly depend on CO_2 availability and the CO_2:O_2 ratio, as both CO_2/O_2 compete for catalytic site of Rubisco. Green alga *Chlamydomonas reinhardtii*, can overcome CO_2 shortage by inducing CO_2-concentrating mechanism (CCM). Cells transferred to low-CO_2 are subjected to light-driven oxidative stress due to decrease in the electron sink. Response to environmental perturbations is mediated to some extent by changes in the lipid and carotenoid metabolism. We thus hypothesize that when cells are challenged with changes in CO_2 availability, changes in the lipidome and carotenoids profile occur. These changes expected to be transient, when CCM is activated, CO_2 limitation will be substantially ameliorated. In our experiments, cells were transferred from high (5%) to low (air equilibrium) CO_2. qPCR analysis of genes related to CCM and lipid metabolism was carried out. Lipidome was analyzed both in whole cells and in isolated lipid droplets. We characterized the changes in polar lipids, fatty acids and ketocarotenoids. In general, polar lipids significantly and transiently increased in lipid droplets during CCM. Similar pattern was observed for xanthophylls, ketocarotenoids and their esters. The data supports our hypothesis about the roles of lipids and carotenoids in tackling the oxidative stress associated with acclimation to sub-saturating CO_2.

1. Introduction

Long and short term carbon (C) and energy budgets of photosynthetic organisms are strongly dependent on CO_2:O_2 ratios. This is due to the fact that CO_2 and O_2 compete for the active site of ribulose-1,5-bisphosphate carboxylase/oxygenase (Rubisco), the enzyme responsible for CO_2 fixation. The relative proportions of carboxylation and oxygenation determine the overall rate and the cost of C fixation [1]. Long term changes in the CO_2: O_2 ratio have exerted a strong selective pressure on photosynthetic organisms, which, most likely polyphyletically, have acquired mechanisms to pump CO_2 into the proximity of Rubisco, the so called CO_2 concentrating mechanisms

☆ Short summary: A lipidomic approach to find out the changes in the polar lipids, fatty acids and carotenoids during induction of CO_2-concentrating mechanism in *Chlamydomonas reinhardtii*.

* Correspondence to: A.K. Bajhaiya, Algal Biotechnology Lab, Department of Microbiology, School of Life Sciences, Central University of Tamil Nadu, Thiruvarur, Tamil Nadu 610005, India.

** Correspondence to: T. Moritz, Umeå Plant Science Centre, Department of Forest Genetics and Plant Physiology, Swedish University of Agricultural Sciences, SE 90183 Umeå, Sweden.

E-mail addresses: amitkumar@cutn.ac.in (A.K. Bajhaiya), thomas.moritz@slu.se (T. Moritz).

[1] Authors with equal contribution.

https://doi.org/10.1016/j.algal.2020.102099
Received 4 May 2020; Received in revised form 29 September 2020; Accepted 1 October 2020
Available online 19 October 2020

(CCMs) [2,3].

The unicellular alga *Chlamydomonas reinhardtii* has been used as a model organism for the study of CCMs. The *C. reinhardtii* CCM is a typical biophysical CCM [2,3] which relies on energy-dependent Ci transport systems, a set of carbonic anhydrases (CAs) and the compartmentalization of Rubisco in the pyrenoid [2,3]. In *C. reinhardtii*, as in most microalgae, the CCM is inducible and its activity is down-regulated when CO_2 concentration increases. *C. reinhardtii* expresses the CCM fairly rapidly, although maximum CCM protein expression is observed within a few hours of the transfer from high to low CO_2 [2,4]. Before the CCM is fully activated, cells transferred to low CO_2 show increased photorespiration and symptoms of oxidative stress, probably because of a decrease in the electron sink constituted by CO_2 fixation [5–7]. Changes in both membrane and non-membrane lipid composition are among the consequences of acclimation to sub-saturating CO_2 [5,6,8–10]. This is not surprising, given the importance of lipids for cell functioning, growth and development [11].

In green algae, stressogenic environmental perturbations often elicit the formation of lipid droplets (LDs) [12–14], which are usually linked to the re-shuffling of carbon from carbohydrates to lipids [12]. LDs are important reservoirs of lipids and likely participate in the maintenance of lipid homeostasis. In line with this function, proteins involved in lipid synthesis, signaling and trafficking are found on the surface of LDs [15]. Lipids mobilized from LDs can serve as a source of energy and participate in membrane synthesis, in thylakoid development and in stress-responses [16]. LDs are composed mainly of sterol esters (SE), diacylglycerols (DAGs), triacylglycerols (TAGs) as well as the polar lipid diacylglyceryl-trimethylhomoserine (DGTS), and intermediates in their biosynthesis and catabolism [17,18]. Studies of metabolic pathways leading to fatty acids and TAG biosynthesis in plants and algae have shown that along with lipids, carotenoid production can be altered in stressogenic conditions [12]. Carotenogenesis is enhanced by reactive oxygen species (ROS) produced under severe nutrient deficiency, high light or high salinity. Carotenoids such as β-carotene and astaxanthin can be accumulated in lipid droplets outside the chloroplast [12,19]. This is intriguing, given that carotenoids are part of light-harvesting antennas, act as photoprotectants by quenching singlet oxygen and excited triplets of some molecules and by scavenging free radicals, influence structural and dynamic properties of biomembranes, decrease the susceptibility of membrane lipid to oxidative degradation [20].

Despite the extensive body of research on CCMs and on the pathways of lipid and carotenoid metabolisms in algae, the interaction between CCMs and lipid-carotenoid metabolisms is poorly understood. Acclimation to low CO_2 has been shown to influence carbohydrate [21] and lipid [22] metabolism. In low-CO_2 grown *Chlorella kessleri*, repression of overall fatty acid synthesis and increased synthesis of specific unsaturated fatty acids has been shown [22]. In contrast, studies by Fan et al. [9] suggested that, in *Chlorella pyrenoidosa*, acclimation to low CO_2 induced the accumulation of saturated fatty acids. Previously we have shown that cell number and relative growth of *C. reinhardtii* were not affected until cells had experienced 6 h of limiting CO_2 conditions. However, there was evidence that lipid metabolism could be regulated during early CCM establishment [6]. All these studies have only partially addressed the connection between CCM induction and lipid metabolism. In this study, we aimed at exploring the interaction between acclimation to low CO_2 concentration (via CCM induction) and lipid metabolism, in the green alga *Chlamydomonas reinhardtii.*

2. Material and methods

2.1. Algal strain and culture conditions

The *Chlamydomonas reinhardtii* cell-wall-less mutant CW-92 was pre-cultured in high salt medium (HSM) [23] bubbled with air enriched with 5% CO_2, at 22 ± 2 °C and 220 ± 20 μmol m^{-2} s^{-1} continuous irradiation from cool, white fluorescent lamps (Philips Master TLD 36 W/830). Cells used for lipidomic analysis were taken from pre-culture and were grown in HSM under the same conditions described above until the logarithmic growth phase was reached, which was confirmed by population growth rate estimation based on cells counting under a microscope. For all analyses the cells derived from mid-logarithmic phase were used. Three independent experiments were conducted. For CCM induction the gas stream was changed from 5% to ambient air (0.04% CO_2 - low CO_2). Cultures bubbled with 5% CO_2 (high CO_2) were used as control.

2.2. Induction of CO_2-concentrating mechanism

At the beginning of each experiment, 5%-CO_2-grown cultures that were in logarithmic growth phase were diluted to an optical density at 750 nm (OD_{750}) of 0.95 ± 0.05 and redistributed into 10, 500 mL flasks. To facilitate acclimation to the experimental conditions (to exclude possibility that culture dilution influenced CCM status in the control cells), a 1.5 h interlude with 5% CO_2 bubbling and a light intensity of 220 ± 20 μmol photons m^{-2} s^{1} (Philips Master TLD 36W/830) was included when cultures were subjected to bubbling with ambient air to start CCM induction. To ensure that in the control cultures CCM does not operate and that low-CO_2 cultures fully induced CCM, western-blot analysis was done to detect the low-CO_2-induced mitochondrial carbonic anhydrase protein (mtCA), according to [6]. The mtCA protein could not be detected under non-inducing conditions, although under CCM inducing conditions this transcript was detected. One of the representative Western blots is shown in Supplementary Fig. S1.

Samples were taken from each bottle after 3 h and 6 h since the onset of CCM induction for lipidomics, western-blots, cell counting and OD measurement. Cells were counted with a light microscope using a standard method [24]. Samples for lipidomic analyses were harvested and immediately quenched according to Bolling and Fiehn [25].

2.3. Lipid droplets fraction (LDF) isolation

A fraction containing lipid droplets was isolated following the protocols described by Moellering and Benning [26] and Ytterberg et al. [27] with some modifications. Five low-CO_2 samples were harvested from culture flasks and immediately centrifuged for 5 min at 2500*g*, at room temperature. The supernatant was removed and the pellet resuspended in pre-cooled (on ice) buffer "A" (50 mM HEPES-KOH, pH 8.0; 5 mM $MgCl_2$; 5 mM KCl; 0.5 M sucrose; cocktail of protease inhibitors (Roche Diagnostics)). Cells were then disrupted using a French press (500 bar, 5 °C); the slurry was transferred to ultracentrifuge tubes, overlaid with pre-cooled (5 °C) buffer "B" (buffer "A" without sucrose) and centrifuged (100,000*g*, 30 min, 10 °C). The upper (light-yellow) fraction, containing lipids, was collected, transferred to an ultracentrifuge tube, mixed with pre-cooled (5 °C) buffer "C" (50 mM HEPES-KOH, pH 8,0; 5 mM $MgCl_2$; 150 mM KCl; 0.5 M sucrose; cocktail of protease inhibitors (Roche Diagnostics)) and overlaid first with pre-cooled (5 °C) buffer "D" (buffer "A" with 0.2 M sucrose instead of 0.5 M sucrose) and then with pre-cooled (5 °C) buffer "B". After centrifugation (100,000*g*, 60 min, 10 °C), the yellow fraction of lipid floating on the surface of the water column was collected, immediately frozen and kept at -80 °C until required for analysis.

2.4. Lipid extractions

The pellets of freeze-dried cells or isolated LD were extracted in 200 μl of NaCl (0.05 M) and 1 ml of chloroform:MeOH (2:1, v:v.) containing [$^{2}H_7$]-cholesterol and [$^{13}C_4$]-hexadecanoic acid as internal standards. After incubation (2 h) and centrifugation (4 °C, 5 min, 20,000*g*), 200 μl of the lower phase was transferred to a LC or GC vial then dried in a speed vac. The extracts were kept at -80 °C prior to

analysis. Total lipid extraction and measurements were performed according to Bligh and Dyer [28].

2.5. Free fatty acid analysis of cell extracts

The dry lipid extracts were dissolved in heptane, derivatized and analyzed by gas chromatography combined with time-of-flight mass spectrometry (Pegasus HT GC- TOFMS; LECO Corp., St Joseph, MI, USA). Alkane series (C_8-C_{40}) was included in the analysis for determination of retention indices [29]. (Detailed methodology is described in supplemental method file SM1).

2.6. Lipidomic analysis of cell and lipid droplets fraction

Lipid analysis was performed on an Agilent 1290 Infinity UHPLC-system (Agilent Technologies, Waldbronn, Germany) coupled to a Q-TOF mass spectrometer. 1 μl of LD extract was injected onto an Acquity UPLC CSH (2.1 × 100 mm, 1.7 μm C_{18}) column held at 60 °C. The gradient elution buffers were A (60:40 acetonitrile:water, 10 mM ammonium formate, 0.1% formic acid) and B (90:10 2-propanol:acetonitrile, 10 mM ammonium formate, 0.1% formic acid), and the flow-rate was 0.5 ml min^{-1}. The lipids were detected in positive ion mode, *m/z* range was 100–1700. Mass Feature Extraction (MFE) from the data acquired was performed using the MassHunter™ Qualitative Analysis software package, version B06.00. Extracted features were aligned and matched between samples using Mass Profiler Professional™ 12.5 (Agilent Technologies Inc., Santa Clara, CA, USA).

2.7. Lipid identification

Significant metabolites derived from the statistical analysis were selected for identification. The extracts were analyzed on a LC - LTQ Orbitrap mass spectrometer (Thermo Fischer Scientific; USA) operating in positive ion mode using a data dependent MS2 in which a full scan (*m/z* 100–1500) was followed by fragmentation of the base peak of the resulting mass spectrum. Three strategies were used to identify the classes of lipid and their respective molecular species in the extracts: 1) the high mass accuracy of their fragments produced by higher energy collisional dissociation (HCD) experiments, the presence of diagnostic fragments, adduct forms, sugar neutral loss and retention time; 2) comparison of high mass accuracy and retention time with current literature and available databases; 3) monoisotopic mass predictions of esterification between ketocarotenoids and fatty acids. The identification of the major intact polar lipids (IPL) and their constituent species was based on the presence of diagnostic fragment patterns in the MS2 mass spectra. IPLs with a di- or monoacylglyceryl-trimethylhomoserine (DGTS or AGTS) head group were detected as $[M + Na]^+$or $[M + H]^+$. They produced the diagnostic fragment of *m/z* 236.1496 $(C_{10}H_{22}O_5N)^+$ (Fig. S2A). IPLs with a sulfoquinovosyldiacylglycerol (SQDG) head group were ionized as $[M + NH_4]^+$ and produced a neutral loss of 261 Da ($C_6H_{11}O_8S + NH_4$). Di- and monogalactosyl diacylglycerol (DGDG and MGDG) metabolites gave a diagnostic fragment of *m/z* 243.0842 $(C_9H_{16}O_6Na)^+$, the sodium adduct and the neutral loss of 162 Da. Di- and triacylglycerol were ionized as $[M + NH_4]^+$ or $[M + Na]^+$.

2.8. RNA extraction and quantitative real time PCR analysis

RNA was extracted from cells grown under high and low CO_2 (as described in the *Induction of CO2-concentrating mechanism* section) at 1, 3 and 6 h (after transfer to low CO_2 conditions) using three biological replicates for each time point. Total RNA was extracted using Trizol reagent (Life Technologies) and treated and purified using an RNA mini spin column (Qiagen RNAeasy kit). The quality of the RNA preparations was verified using a BioAnalyzer (BioAnalyzer 2100, Agilent Technologies, USA) and they were quantified by a NanoDrop 2000C UV–Visible spectrophotometer (Thermo Fisher Scientific, USA). Purified RNA was reverse-transcribed using iScript™ cDNA synthesis kit (BioRad, USA). Expression levels of selected genes was determined by quantitative real time PCR (qRT-PCR, Roche LightCycler480) using SYBR Green I Master mix (Roche). Melting curves were generated to confirm that the single product is amplified. The amplification product sizes were between 90 and 120 bp. The relative amplification efficiency of all qPCRs varies between 98% and 99%. *CBLP/RACK1* (Receptor of activated protein kinase C, Phytozome id: Cre06.g278222.t1.1) and *RBCS1* (ribulose-1,5-bisphosphate carboxylase/oxygenase small subunit 1, Phytozome id: Cre02.g120100.t1.2) were used as housekeeping genes to normalize the expression data. The primer pairs used for qPCR expression analysis are listed in Supplementary Table S1. Annotation of genes was according to Phytozome version 12.1.6.

2.9. Statistical analysis

The Cell and LDF datasets from the lipidomic analysis were analyzed by the multivariate projection methods Principal Component Analysis (PCA) and Orthogonal Projections to Latent Structures Discriminant Analysis (OPLS-DA). Valid models were obtained independently for each of the three experiments performed on cells, comparing High CO_2 (H-CO_2) and Low CO_2 (L-CO_2) after 3 and 6 h (Table S2-A). A similar comparison was performed for the LDF dataset: OPLS-DA was performed on the entire dataset (831 features) and valid models could discriminate between LDF from H-CO_2 and L-CO_2 after 3 and 6 h (Table S2-B). Lipids distinguishing the samples were identified using the OPLS-DA loading plots. In all cases, models were judged for quality using the goodness of fit (R^2X) and goodness of prediction (Q^2) parameters. R^2X values vary between 0 and 1 (i.e. they describe 0–100% of the variation in the data). The total explained variance in Y is R^2Y (0–1). The predictive ability of the model according to cross-validation is the Q^2 value (0–1) where 1 equals perfect predictivity. All multivariate analyses were performed using SIMCA-P + 14 (Umetrics AB, Umeå, Sweden).

OPLS-DA was performed on the dataset generated from the levels of expression of 47 genes analyzed by RT–PCR at each time point (1, 3 and 6 h) comparing H-CO_2 and L-CO_2 (Table S2-C). The bi-plot (score x loading plot) of the valid models for each time point was scaled as correlation and the threshold ± 0.5 was used to select significant transcripts. P(corr) values from the loading plots were listed and a heatmap was built to provide better visualization of the results using MATLAB R2014b software.

3. Results

3.1. Changes in lipid composition of entire cells under limiting CO_2 conditions

To test whether the lipid content is modified under limiting CO_2 conditions, we measured total lipids from *C. reinhardtii* cultures grown under high CO_2 (H-CO_2) or low CO_2 (L-CO_2) for 3 and 6 h. We did not observe any significant changes in total lipid content after 3 or 6 h of L-CO_2 treatment compared to H-CO_2 (Fig. S3).

Furthermore, the free fatty acid composition was analyzed in the extracts from entire cells using GC–MS (Fig. S4). Significant changes were observed in free fatty acid composition during CCM establishment at 3 h and that stage the levels of $C_{16:0}$, $C_{18:0}$, $C_{18:3}$, $C_{18:4}$ and $C_{17:1}$ increased, while the levels of $C_{16:2}$, $C_{16:3}$ and $C_{18:2}$ were reduced. Interestingly, the fatty acids derived from hexadecanoic acid ($C_{16:0}$) and $C_{18:2}$were present at reduced levels in the cells grown under L-CO_2 at 6 h.

From the lipidomic approach applied to cell extracts, we found lipids significantly differ between L-CO_2 and H-CO_2; among them were DGTS, MGDG, SQDG, DAG and TAG (Table S3). Changes in DGTS were more pronounced than those in MGDG, DAG, SQDG and TAG. The

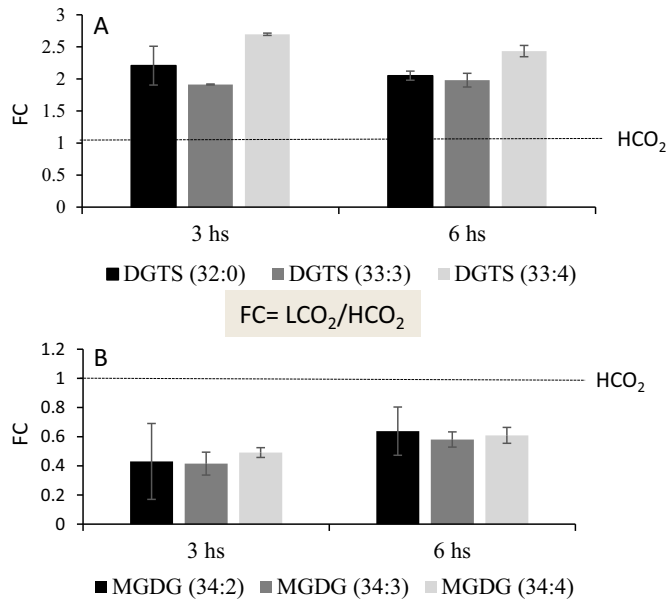

Fig. 1. Changes in Diacylglyceryl-trimethylhomoserine (DGTS) (A) and Monogalactosyldiacylglycerol (MGDG) (B) in *C. reinhardtii* cells after 3 and 6 h under limiting CO_2 conditions. Data is expressed as fold changes (FC) of the mean values (three independent experiments, n = 10), of low CO2 in relation to control conditions (LCO2/HCO2) ± SD. Relative control level (HCO2) is shown as a line.

levels of DGTS ($C_{32:0}$) containing saturated species of hexadecanoyl (C_{16}) in both *sn*-glycerol backbones showed a two-fold increase under L-CO_2. Similarly, levels of DGTS containing heptadecanoyl (C_{17}) and nonadecanoyl (C_{19}) (DGTS 33:3 and 35:4) increased up to 2.7 and 1.5 times respectively compared to the contents of the H-CO_2 cells (Fig. 1A). The presence of these odd chain length molecular species (C_{17} and C_{19}) was confirmed by the fragments *m/z* 486.3782 (C_{27} H_{52} O_6 N)$^+$ and *m/z* 514.4083 (C_{29} H_{56} O_6 N)$^+$ in MSMS experiments.

The levels of MGDG, which is the most abundant class of lipids present in *C. reinhardtii* cells, were altered under L-CO_2 conditions. MGDG ($C_{34:2–4}$) decreased in cells grown under L-CO_2 conditions for 3 and 6 h (Fig. 1B). Interestingly, we did not detect any changes in MGDG ($C_{34:7}$), an important chloroplast membrane component [30]. However, SQDG ($C_{32:0}$) was slightly increased after 6 h under L-CO_2 treatments (Table S3).

Although several studies have shown the accumulation of TAG under adverse conditions [31,32], we found inconsistent results between the three experiments. So, in order to enhance their levels, we decided to analyze the lipid droplets isolated from *C. reinhardtii* cells grown under similar experimental conditions.

3.2. Lipid accumulation in lipid droplets under limiting CO_2 conditions

Lipid droplets fraction (LDF) was isolated from cells grown under H-CO_2 and L-CO_2 conditions for 3 and 6 h. In analysis of these samples, TAG, DAG, DGTS and AGTS were the most abundant glycerolipids detected (Table 1). In contrast to the whole cell extracts, more consistent changes in TAG levels were observed in LDF. TAG containing the acyl combinations C_{48}, C_{50}, C_{52} and C_{54}, DGTS containing C_{32}, C_{33} and C_{34} and DAG ($C_{34:2–3}$) increased in the first 3 h under L-CO_2 conditions, and then returned to levels similar to those of cells grown in control conditions (H-CO_2) after 6 h (Fig. 2A–H and J).

3.3. Carotenogenesis under limiting CO_2 conditions

Apart from glycerolipids, the level of carotenoid related metabolites (xanthophylls and ketocarotenoids) also changed significantly under L-CO_2 conditions (Fig. 3). In the biosynthetic pathway, β-carotene is a precursor of zeaxanthin - the component of the xanthophyll cycle, which can be converted into antheraxanthin and further to violaxanthin [33]. Both zeaxanthin and violaxanthin accumulated in the LDF during the first 3 h under L-CO_2, returning to levels similar to those of control cells (H-CO_2) after 6 h. Further oxidation steps of zeaxanthin and violaxanthin can lead to the biosynthesis of either astaxanthin (Ast) or 5,6-epoxy-3-hydroxy-12′-apo-β-carotene-12′-al (EAC) respectively. Astaxanthins, but not EAC, accumulated in LDF after 3 h under L-CO_2 (Fig. 3). This result suggests that the metabolic pathway in the direction of Ast was favored during the early stage of CCM establishment (3 h), resulting in 5-fold accumulation of Ast in the LDF. In contrast, the biosynthetic pathway towards EAC became more active after 6 h under L-CO_2, when the CCM was established. The precursor of β-carotene, *trans*-lycopene can also be directed to oxidation steps resulting in different forms of oxo-spirilloxanthin (SP). These SP forms also accumulated in the LDF during the first 3 h under L-CO_2. Like Ast, the SP levels returned to normal after 6 h (Fig. 3).

Astaxanthin and SP are stored mainly in lipid droplets and can be esterified with fatty acids. Such esterification takes place in the ER prior to transport to LDs [34]. Esterified forms of ketocarotenoids (Ast and SP) with $C_{16:0}$, $C_{16:3}$, $C_{18:0}$ and $C_{18:2–18:4}$ were detected and characterized in the LDF extracts. The annotations were based on identification of the neutral loss of acyl group in the MSMS spectra (Fig. S2B). Accumulation of Ast- and SP-fatty acid esters was observed in the LDF during CCM establishment (3 h under L-CO_2); most of these compounds returned to control levels after 6 h (Fig. 4), similarly to what was observed for xanthophylls and glycerolipids (Figs. 2 and 3).

3.4. Impact of limiting CO_2 conditions on gene expression related to lipid metabolism

To confirm the lipidomic results, we carried out a quantitative reverse transcription PCR (qRT-PCR) analysis of 56 genes related to CCM and lipid metabolism (Table S4) at 1, 3 and 6 h after cells were transferred from H-CO_2 to L-CO_2. First, we analyzed the transcript levels for seven low CO_2 induced genes, out of which three of them (*CCP1*, *CCP2* and *HLA3*) are known to have direct role in CCM, whereas other four (*CAH4*, *CAH5*, *LCI 1*, *LCIA/NAR1.2*) are known to be expressed under LCO_2 conditions ([35–38]). Two mitochondrial beta-CA genes (*CAH4* and *CAH5*), an LCO_2-inducible membrane protein (*LCI1*), two chloroplast envelope proteins (*CCP1* and *CCP2*), and two HCO_3 transporters (*HLA3*, *LCIA/NAR1.2*) were analyzed. Although both *CCP1/2* are still named as chloroplast envelope protein on Phytozome but their association with mitochondria is already shown in *C. reinhardtii* and tobacco [39]. Under our experimental conditions, all of these marker genes were highly upregulated after 1, 3 and 6 h of L-CO_2 (Fig. S5). These results confirm that the CCM was induced and established during our experimental conditions.

The expression levels of genes related to lipid metabolism (Table S4) were analyzed in order to investigate whether levels of lipid metabolism gene transcripts could account for the significant changes in lipid composition observed under CCM. The results of transcript level analysis were further analyzed by OPLS-DA, and the data from the valid models were visualized with a combined score-loading bi-plot (Fig. 5A) and as a heatmap (Fig. 5B). The heatmap derived from the OPLS-DA biplot shows that the transcript levels of several genes were affected differently across the sampling time points during exposure to the L-CO_2 conditions. After 1 h under L-CO_2 conditions about 48% of the genes analyzed in our experimental set-up already showed changes in transcript levels (Fig. 5C). After 3 h, expression of 34% of the genes had changed but thereafter the percentage of changes increased to similar numbers as after 1 h of L-CO_2. Interestingly, 26% of the genes showed decreases in their transcription levels after 1 h, 10% after 3 h and only 2% after 6 h (Fig. 5C). Overall, this suggests that changes in the transcription of genes associated with lipid metabolism are correlated with

Table 1
Lipids annotated in lipid droplets isolated from *Chlamydomonas reinhardtii* cultures grown under limiting CO_2 conditions.

Annotation	RT	Adduct	*m/z*	*m/z* (calc)	Δ*m/z*	[M]	Formula
Betaine lipids							
AGTS (16:0)	2.00	[M + H]	474.3797	474.3789	0.0008	473.3711	$C_{26}H_{51}O_6N$
AGTS (18:3)	1.30	[M + H]	496.3619	496.3632	−0.0013	495.3554	$C_{28}H_{49}O_6N$
AGTS (18:1)	2.00	[M + H]	500.3954	500.3945	0.0009	499.3867	$C_{28}H_{53}O_6N$
AGTS (18:0)	3.00	[M + H]	502.4096	502.4102	−0.0006	501.4023	$C_{28}H_{55}O_6N$
DGTS (32:4)	4.4/4.6	[M + H]	704.5503	704.5459	0.0044	703.5381	$C_{42}H_{73}O_7N$
DGTS (32:3)	5.0/5.2	[M + H]	706.5631	706.5616	0.0015	705.5538	$C_{42}H_{75}O_7N$
DGTS (32:2)	5.50	[M + H]	708.5807	708.5772	0.0035	707.5694	$C_{42}H_{77}O_7N$
DGTS (32:1)	6.00	[M + H]	710.5955	710.5929	0.0026	709.5851	$C_{42}H_{79}O_7N$
DGTS (34:4)	5.10	[M + H]	732.5817	732.5772	0.0045	731.5694	$C_{44}H_{77}O_7N$
DGTS (34:3)	5.6/5.80	[M + H]	734.5969	734.5929	0.004	733.5851	$C_{44}H_{79}O_7N$
DGTS (34:2)	6.00	[M + H]	736.6107	736.6085	0.0022	735.6007	$C_{44}H_{81}O_7N$
DGTS (34:1)	6.70	[M + H]	738.6279	738.6242	0.0037	737.6164	$C_{44}H_{83}O_7N$
DGTS (36:7)	4.1/4.2	[M + H]	754.5655	754.5616	0.0039	753.5538	$C_{46}H_{75}O_7N$
DGTS (36:6)	5.4/5.6	[M + H]	756.5811	756.5772	0.0039	755.5694	$C_{46}H_{77}O_7N$
DGTS (36:5)	4.9/5.0	[M + H]	758.5972	758.5929	0.0043	757.5851	$C_{46}H_{79}O_7N$
DGTS (36:4)	5.5/5.7	[M + H]	760.613	760.6085	0.0045	759.6007	$C_{46}H_{81}O_7N$
DGTS (36:3)	6.0/6.5	[M + H]	762.6282	762.6242	0.004	761.6164	$C_{46}H_{83}O_7N$
Di/triacylglycerol							
DAG (34:8)	4.30	[M + NH4]	598.4469	598.4466	0.0003	580.4123	$C_{37}H_{59}O_5N$
DAG (34:7)	4.70	[M + NH4]	600.4626	600.4622	0.0004	582.4284	$C_{37}H_{61}O_5N$
DAG (34:6)	5.00	[M + NH4]	602.4778	602.4779	−1E−04	584.4441	$C_{37}H_{63}O_5N$
DAG (34:5)	5.5/5.8	[M + NH4]	604.4936	604.4935	1E−04	586.4597	$C_{37}H_{65}O_5N$
DAG (34:4)	6.10	[M + NH4]	606.5097	606.5092	0.0005	588.4754	$C_{37}H_{67}O_5N$
DAG (34:3)	6.7/6.9	[M + NH4]	608.5251	608.5248	0.0003	590.4910	$C_{37}H_{69}O_5N$
DAG (34:1)	7.90	[M + NH4]	612.556	612.5561	−1E−04	594.5223	$C_{37}H_{73}O_5N$
DAG (36:4)	6.9/7.1	[M + NH4]	634.5407	634.5405	0.0002	616.5067	$C_{39}H_{71}O_5N$
DAG (36:3)	7.70	[M + NH4]	636.5566	636.5561	0.0005	618.5223	$C_{39}H_{73}O_5N$
TAG (50:11)	8.10	[M + NH4]	830.6316	830.6293	0.0023	812.5955	$C_{53}H_{83}O_6N$
TAG (50:10)	8.80	[M + NH4]	832.6446	832.6449	−0.0003	814.6111	$C_{53}H_{85}O_6N$
TAG (50:9)	8.95	[M + NH4]	834.6612	834.6606	0.0006	816.6268	$C_{53}H_{87}O_6N$
TAG (50:8)	9.6/9.7	[M + NH4]	836.6747	836.6762	−0.0015	818.6424	$C_{53}H_{89}O_6N$
TAG (50:7)	10.10	[M + NH4]	838.6953	838.6919	0.0034	820.6581	$C_{53}H_{91}O_6N$
TAG (50:6)	10.60	[M + NH4]	840.7065	840.7075	−0.001	822.6737	$C_{53}H_{93}O_6N$
TAG (50:5)	10.90	[M + NH4]	842.7238	842.7232	0.0006	824.6894	$C_{53}H_{95}O_6N$
TAG (50:4)	11.30	[M + NH4]	844.7402	844.7388	0.0014	826.7050	$C_{53}H_{97}O_6N$
TAG (50:3)	11.80	[M + NH4]	846.7545	846.7545	0	828.7207	$C_{53}H_{99}O_6N$
TAG (50:2)	12.20	[M + NH4]	848.7713	848.7701	0.0012	830.7363	$C_{53}H_{101}O_6N$
TAG (50:1)	12.60	[M + NH4]	850.7886	850.7858	0.0028	832.7520	$C_{53}H_{103}O_6N$
TAG (52:11)	8.70	[M + NH4]	858.6623	858.6606	0.0017	840.6268	$C_{55}H_{87}O_6N$
TAG (52:10)	9.0/9.2	[M + NH4]	860.677	860.6762	0.0008	842.6424	$C_{55}H_{89}O_6N$
TAG (52:9)	9.1/9.6	[M + NH4]	862.6916	862.6919	−0.0003	844.6581	$C_{55}H_{91}O_6N$
TAG (52:8)	9.90	[M + NH4]	864.7079	864.7075	0.0004	846.6737	$C_{55}H_{93}O_6N$
TAG (52:7)	10.5/10.7	[M + NH4]	866.722	866.7232	−0.0012	848.6894	$C_{55}H_{95}O_6N$
TAG (52:6)	11.0/11.1	[M + NH4]	868.7389	868.7388	1E−04	850.7050	$C_{55}H_{97}O_6N$
TAG (52:5)	11.30	[M + NH4]	870.756	870.7545	0.0015	852.7207	$C_{55}H_{99}O_6N$
TAG (52:4)	11.70	[M + NH4]	872.7717	872.7701	0.0016	854.7363	$C_{55}H_{101}O_6N$
TAG (54:7)	11.30	[M + NH4]	894.7567	894.7545	0.0022	876.7207	$C_{57}H_{99}O_6N$
TAG (54:6)	11.60	[M + NH4]	896.7706	896.7701	0.0005	878.7363	$C_{57}H_{101}O_6N$
Xanthophylls/ketocarotenoids							
Violaxanthin	2.21	[M + H]	601.4246	601.4251	−0.0005	600.4168	C40 H56 O4
Zeaxanthin	5.21	[M + H]	569.4353	569.4353	0	568.4275	C40 H56 O2
5,6-Epoxy-3-hydroxy-12′-apo-β-caroten-12′-al	3.66	[M + H]	409.2738	409.2737	1E−04	408.266	C27 H36 O3
β-Cryptoxanthin	8.39	[M + H]	553.4393	553.4403	−0.001	552.4315	C40 H56 O
15-*cis*-phytoene	7.97	[M + H]	545.5081	545.508	1E−04	544.5003	C40H64
Ast_2: (3S, 3′S) 7,8,7′,8′-tetradehydroastaxanthin	4.18	[M + H]	593.361	593.3625	−0.0015	592.3552	C_{40} H_{48} O4
Ast_3: (3S, 3′S) 7,8-didehydroastaxanthin	4.54	[M + H]	595.377	595.3781	−0.0011	594.3709	C40 H50 O4
Ast_4: (3S, 3′S) astaxanthin	5.09	[M + H]	597.391	597.3938	−0.0028	596.3865	C40 H52 O4
SP1: 2,2′-dioxospirilloxanthin	5.53	[M + H]	625.424	625.4251	−0.0011	624.4178	C42 H56 O4
SP2: 2-oxo-2′-hydroxyspirilloxanthin	6.49	[M + H]	627.439	627.4407	−0.0017	626.4335	C42 H58 O4
SP3: 2,2-dihydroxyspirilloxanthin	7.14	[M + H]	629.455	629.4564	−0.0014	628.4491	C42 H60 O4
Ketocarotenoid esters							
Ast 3_16:0	10.76	[M + H]	833.6061	833.6078	−0.0017	832.5983	C56 H80 O5
Ast 4_16:0	11.35	[M + H]	835.6217	835.6235	−0.0018	834.6162	C56 H82 O5
Ast 3_16:3	9.40	[M + H]	827.5602	827.5609	−0.0007	826.5536	C56 H74 O5
Ast 2_18:3	9.03	[M + H]	853.5756	853.5765	−0.0009	852.5692	C58 H76 O5
Ast 4_18:4	9.63	[M + H]	855.5915	855.5922	−0.0007	854.5849	C58 H78 O5
Ast 4_18:3	10.25	[M + H]	857.6071	857.6078	−0.0007	856.6005	C58 H80 O5
Ast 4_18:2	10.26	[M + H]	859.6228	859.6235	−0.0007	858.6162	C58 H82 O5
SP 3_16:3	11.47	[M + H]	861.6378	861.6391	−0.0013	860.6318	C58 H84 O5
SP 3_16:0	12.92	[M + H]	867.685	867.6861	−0.0011	866.6788	C58 H90 O5
SP 2_17:0	12.24	[M + H]	879.687	879.6861	0.0009	878.6788	C59 H90 O5
SP 2_18:2	11.92	[M + H]	889.6691	889.6704	−0.0013	888.6631	C60 H88 O5

(*continued on next page*)

Table 1 (*continued*)

Annotation	RT	Adduct	*m/z*	*m/z* (calc)	Δ*m/z*	[M]	Formula
SP 2_18:3	12.42	[M + H]	891.6851	891.6861	−0.001	890.6788	C60 H90 O5
SP 2_18:0	12.88	[M + H]	893.7018	893.7017	1E−04	892.6944	C60 H92 O5
SP 3_18:0	13.21	[M + H]	895.7168	895.7174	−0.0006	894.7101	C60 H94 O5

CCM establishment.

Statistically significant differences (*t*-test, $p < 0.05$; see Table S5 for relative expression and *p* values) were obtained for transcripts encoding desaturases, acyl transferases, ligases, lipases and plastidial oxidases, as well as those of genes encoding enzymes that are part of the photorespiration cycle and fatty acid, glycerolipid and carotenoid biosynthesis (Fig. 5D).

We detected rapid changes in the gene expression associated with FAD desaturases, where decreased expression of *FAD6* and *G6252.t* (also known as *FAD2*) were already observed in the first hour under L-CO_2, followed by increased expression of *G6252.t1* and *FAD5C* at 3 h and 6 h.

FAD desaturases are reported to be chloroplast localized and may be related to the synthesis of Δ4 and Δ5 polyunsaturated (PUFA) fatty acids. *FAD6* encodes an isoform of omega-6-fatty acid desaturase known to act upon MGDG (to generate 16:2 and 18:2 fatty acids) and on the SQDG oleate attached to the *sn1* glycerol backbone [30]. The rapid decrease in its expression after 1 h of L-CO_2 is in line with the accumulation of C16:0 and C18:0 as well as the decreased levels of their desaturated molecular species after 3 h of L-CO_2 (Fig. S4).

PGD1 has been shown to be involved in the acyl editing or turnover of galactoglycerolipids during TAG formation in *C. reinhardtii* [40]. The increased expression of *PGD1* during the first hour under L-CO_2 and reduced levels of MGDG after 3 and 6 h of L-CO_2 (Fig. 1B) suggest that galactolipids could be substrates for this lipase.

3.5. CO_2 limiting conditions induce expression of carotenoid biosynthesis genes

We then tested whether changes in expression of carotenoid biosynthesis genes could account for the regulation of carotenogenesis under CCM establishment. While we observed reduced transcript level of *VDR* (violaxanthin synthase) after 1 h and of *CYP97A5* (carotenoid hydroxylase) after 3 h of L-CO_2, *CYP97 A6* transcripts were upregulated at all three time points. This is consistent with the accumulation of astaxanthin and spirilloxanthins in the LDF (Fig. 3). Under L-CO_2 conditions we observed a tendency for upregulation of *PTOX2* after 3 and 6 h of L-CO_2 (although this was not statistically significant), contrasting with previously published results from *H. pluvialis*, in which the transcription of *PTOX1* was positively correlated with accumulation of Ast [14].

Enzymes from the DGAT gene family are known to catalyze the acyl-esterification of diacylglycerol (DAG) resulting in TAG [30]. The esterification of astaxanthin produced in *H. pluvialis* cells under stress conditions is also mediated by DGAT enzymes [41]. However, in our study the transcription of DGAT family genes (*DGTT3* and *4*) was downregulated under L-CO_2 conditions (Fig. 5). In contrast, increased transcripts levels for *LCL1* (long chain fatty acyl-CoA ligase) [42] were observed at all time points in our experimental setup. Proteome analyses indicated the presence of LCL1 in lipid droplets, suggesting an active role for LCL1 in TAG synthesis [30]. The accumulation of Ast has been closely associated with TAG biosynthesis during carotenogenesis [34]. This is in line with our findings that TAG and Ast/SP-acyl accumulate in LDF during CCM induction. The combined results from the lipidomic and qPCR analysis suggests that the transcriptional regulation

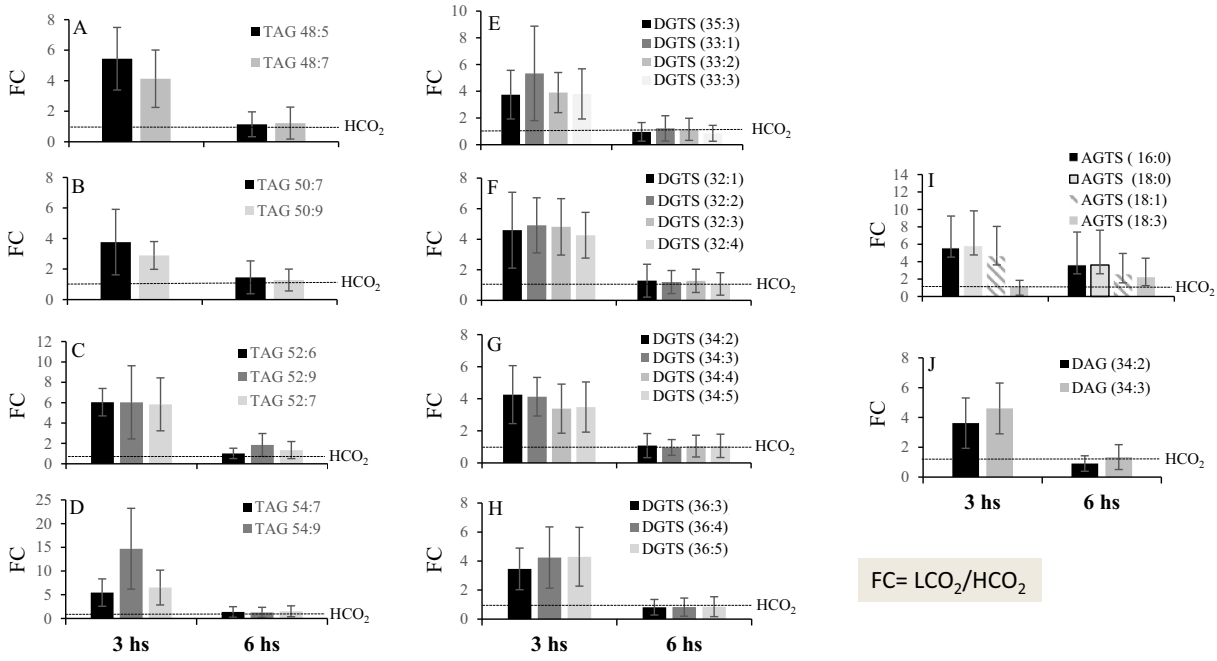

Fig. 2. Changes in lipid composition in lipid droplets fraction (LDF) isolated from *C. reinhardtii* cells grown under limiting CO_2 conditions at 3 and 6 h: A–D: Triacylglycerols (TAGs); E–H: Diacylglyceryl-trimethylhomoserine (DGTS); I: Monoacylglyceryl-trimethylhomoserine (AGTS); J: Diacylglycerols (DAGs). Data is expressed as fold change (FC) of the mean value (n = 5) of low CO2 in relation to the control conditions (HCO2) ± SD. Relative control level (HCO2) is shown as a line.

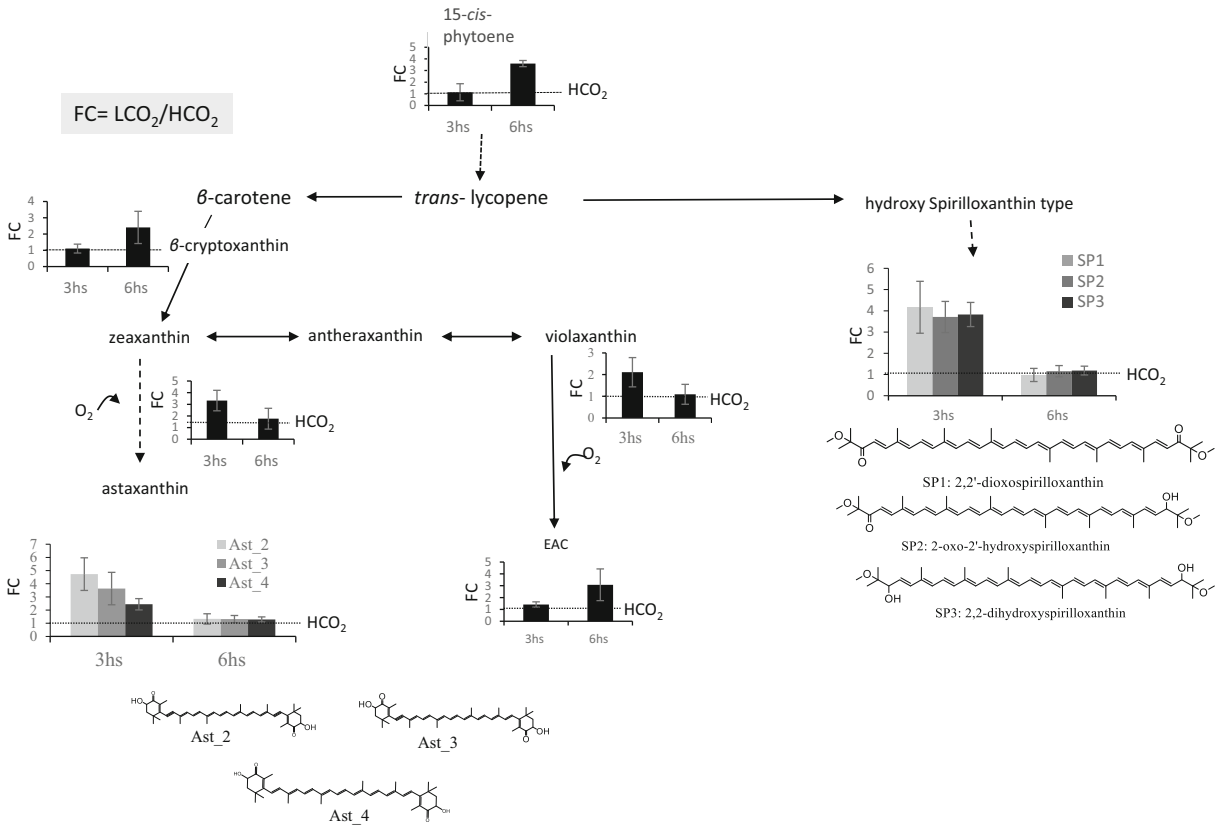

Fig. 3. Overview of xanthophylls and ketocarotenoids changes in lipid droplets fraction (LDF) isolated from *C. reinhardtii* cells grown under limiting CO_2 conditions. Ast_2 (7,8,7′,8′-Tetradehydroastaxanthin); Ast_3 (7,8-Didehydroastaxanthin); Ast_4 (astaxanthin); SP1 (2,2′-dioxospirilloxanthin); SP2 (2-oxo-2′-hydroxyspirilloxanthin); SP3 (2,2-dihydroxyspirilloxanthin); EAC (5, 6-epoxy-3-hydroxy-12′-apo-β-caroten-12′-al). Data is expressed as fold change (FC) of the mean value (n = 5) of low CO2 in relation to the control conditions (HCO2) ± SD. Relative control level (HCO2) is shown as a line.

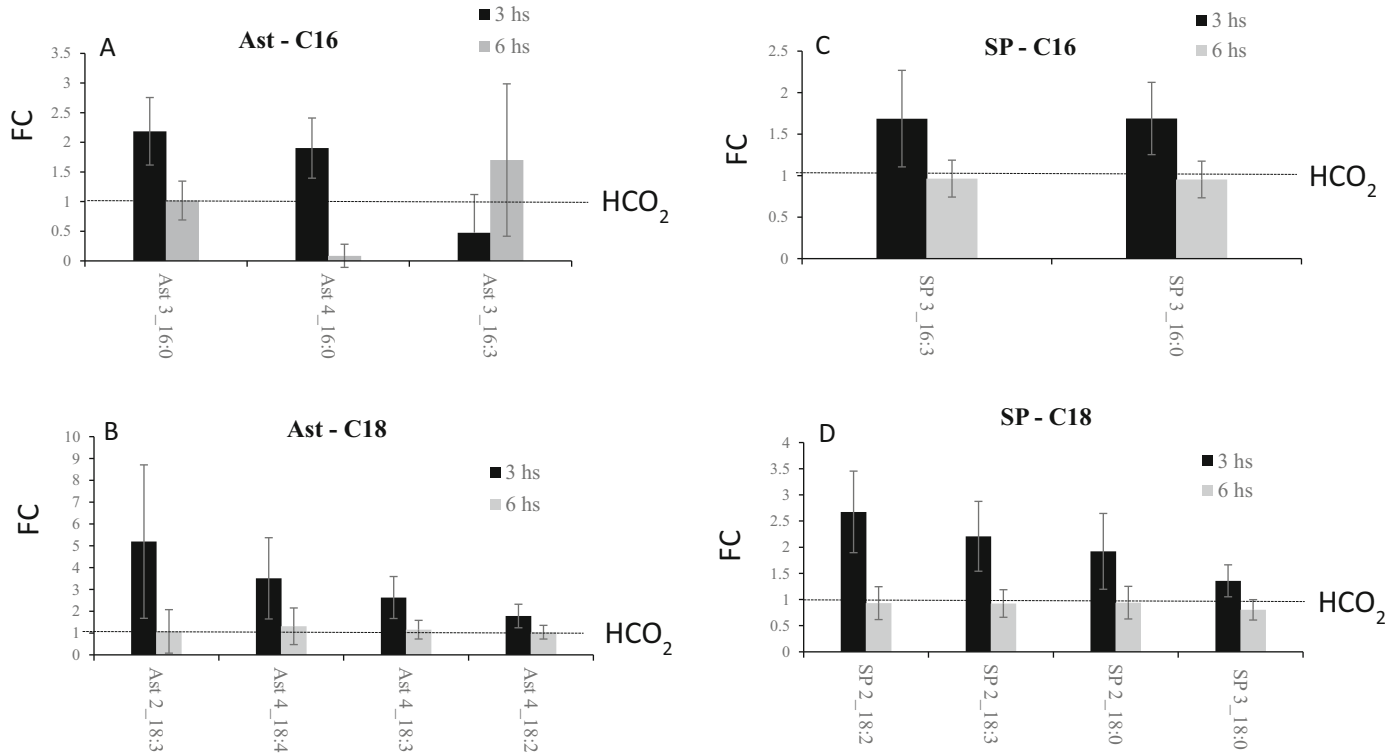

Fig. 4. Ketocarotenoid-esters changes in lipid droplets fraction isolated from *C. reinhardtii* cells grown under limiting CO_2 conditions. A) Astaxanthin- C16; B) Astaxanthin – C18; C) oxospirilloxanthin -C16; D) oxospirilloxanthin- C18. Data is expressed as fold change (FC) of the mean value (n = 5) of low CO2 in relation to the control conditions (HCO2) ± SD. Relative control level (HCO2) is shown as a line.

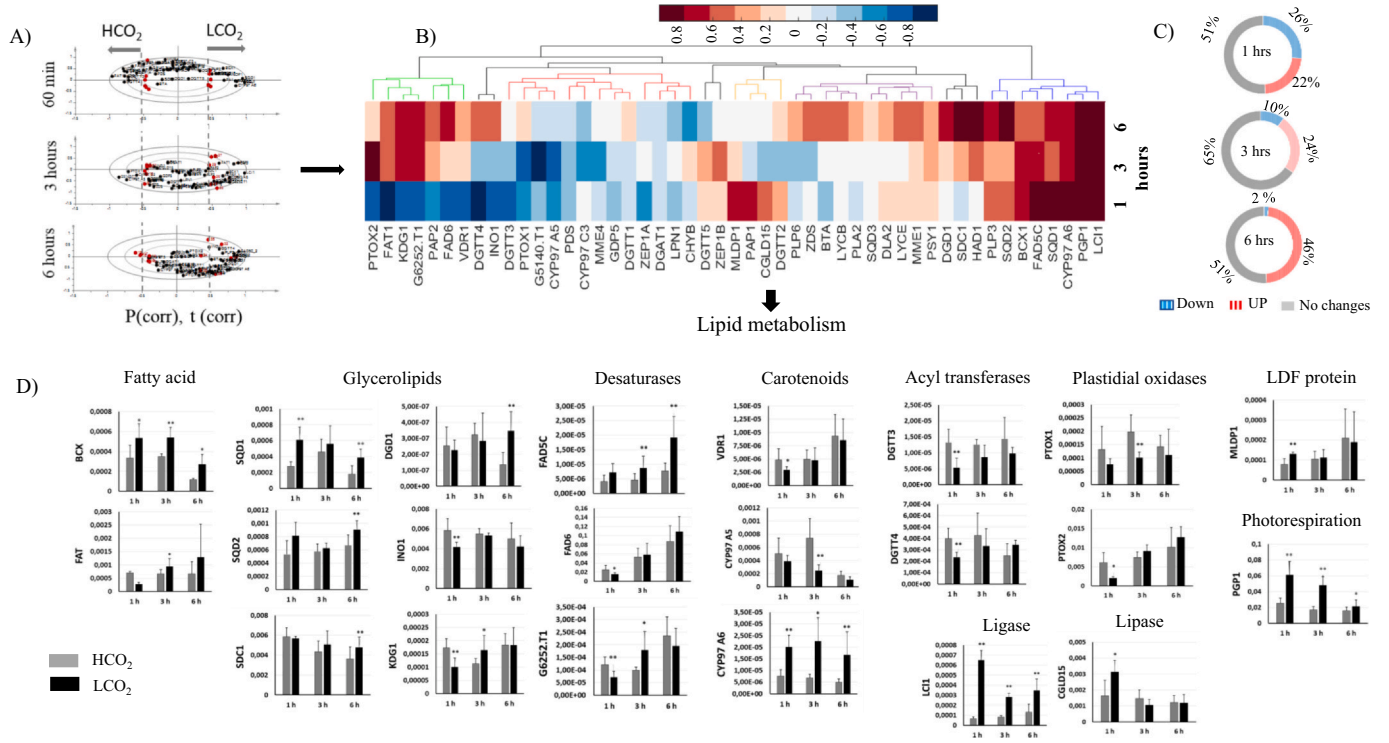

Fig. 5. Impact of limiting CO_2 conditions on expression of *C. reinhardtii* lipid metabolism related genes – A) HeatMap based on P(corr) from the OPLS-DA Bi-plots of 49 genes under high and low CO_2 at 1, 3 and 6 h; B) percentage of genes that were up-regulated (red), down-regulated (blue) or no changes (grey) in the OPLS-DA; C) Illustration of the relative expression of the significant genes (classified accordingly to their enzyme functions in lipid metabolism); data represent mean values (n = 6) ± SD; asterisks mean significant differences (*t*-test) at $p < 0.05$ (*) or $p < 0.01$ (**). The relative expression levels of different genes analyzed in this work and their respective *p* values are available in Table S5.

of lipid and carotenoid biosynthesis genes can, to a certain extent, explain changes in lipid composition during CCM establishment.

4. Discussion

Carbon concentrating mechanisms (CCMs) are crucial for algal cells when the CO_2 concentration is insufficient to saturate Rubisco [2,43]. During CCM induction, the expression of several genes encoding carbonic anhydrases (CAs), bicarbonate transporters [44], and other low-CO_2 induced (*LCI*) genes are modulated [39]. However, transcriptome data obtained from *C. reinhardtii* and *Cyanophora paradoxa* indicate that during CCM establishment a set of stress-response genes are also up-regulated, probably due to the oxidative stress to which cells are exposed after transfer to L-CO_2 conditions because of the reduced capacity of CO_2 fixation to act as electron acceptor [6,8,35]. It has been known for many years that CO_2 is limiting for electron transport under most "natural" conditions, and that the regulation of electron transport between photosystems II and I is sensitive to the availability of CO_2 [45]. The rate of electron transport under low CO_2 can be down-regulated up to 50% relative to the maximum rate achievable in saturating CO_2 and this down-regulation can be explained by regulation of the electron transport chain itself, e.g. via CO_2-limitation at the level of Rubisco, which decrease the overall flux through the Calvin cycle [45]. Furthermore, low chloroplastic CO_2/O_2 ratio and/or reduced cell capacity to assimilate CO_2 has been shown to cause an increase in photosynthetic electron flux to O_2, resulting in the increased production of superoxide, H_2O_2, and hydroxyl radicals [46–49]. On the other hand, high CO_2 has been reported to promote both PS II and PS I photochemistry under stress conditions, by alleviating the limitations in both donor and acceptor sides of the photosystems and preventing ROS overproduction [50].

When cells are transferred from H-CO_2 to L-CO_2, a temporary stimulation of photorespiration is expected. Before the CCM is fully induced, the intracellular CO_2:O_2 ratio is too low to saturate Rubisco with CO_2 thus Rubisco catalyzes oxygenation of ribulose-1,5-bisphoshate, with the production of 2-phosphoglycolate (2-PGL) [6], which after dephosphorylation by 2-phosphoglyolate phosphatase (PGP) is further metabolized in *C. reinhardtii* mitochondria to recover part of the C allocated to 2-PGL [51]. In our study, the expression of *PGP1* was increased and its increased expression was still observed after 6 h of the L-CO_2 treatment; this may indicate that full CCM induction requires more time than is necessary for the abundance of CCM marker gene transcripts to reach a steady state (Fig. S5). This is in line with our previous report that major differences in metabolites between H-CO_2 and L-CO_2 cells can persist until 12 h after the CCM is induced [6]. Furthermore, we were able to analyze in detail the changes in lipid metabolism that were briefly referred by Renberg et al. [6], in order to elucidate the role of lipid remodeling in L-CO_2 acclimation.

A characteristic feature of the *C. reinhardtii* membranes is the lack of phosphatidylcholine (PtdCho), which in embryophytes is a key intermediate in the endoplasmic-reticulum (ER) pathway of lipid synthesis [52]. In *C. reinhardtii*, PtdCho is replaced by the non-phosphorus betaine lipid DGTS [30]. DGTS is found mainly in non-plastidial membranes, with much smaller amounts detected in the plastid fraction, where it is believed to play the same role as the PtdCho in plant outer chloroplast envelopes [53]. The lack of PtdCho may be the reason why in *C. reinhardtii* chloroplast lipids are synthetized mainly in plastids [18]. Here, we detected plastid MGDG, DGDG and SQDG containing C_{16} in the *sn2-position* of the glycerol backbone, a feature typical of lipids derived from the plastid biosynthetic pathway [30]. Although the glycerolipid composition of photosynthetic membranes is believed to be evolutionally conserved [54], the photosynthetic apparatus must undergo fast lipid turnover in response to environmental perturbation. During high to low CO_2 transition we observed a decrease in total MGDG, whereas DGDG and SQDG did not show noteworthy variations (Fig. 1, Table S3). These polar membrane lipids have different phase

properties with water, DGDG and SQDG are lamellar (L) and MGDG is a hexagonal II (HII) phase lipid respectively. The general role of the HII lipid is to give the membrane a high internal lateral pressure among the fatty acyl chains and a pressure on the membrane proteins [55]. Due to the non-bilayer lipid properties of MGDG, different ratios of DGDG/MGDG will affect the lateral pressure on membrane proteins [55], and thereby might affect the photosynthetic apparatus, as have been shown e.g. in *Arabidopsis* with reduced MGDG levels [56–58]. Furthermore, it has been shown that a lower DGDG/MGDG ratio reflects increased sensitivity of *C. reinhardtii* to environmental stressors, e.g. high salinity or low temperature [53]. Here, the DGDG/MGDG ratio increased due to the decrease in MGDG, which can be a manifestation of stressogenic effect caused by photosynthesis reduction during L-CO_2 acclimation [46–49]. The above is in a line with the results of meta-analysis reported by Xiaoxiao et al. [58] that under various abiotic stresses, such as salt, low temperature and drought stresses, the DGDG/MGDG ratio in plant cells changes, mainly due to the more pronounced decrease in MGDG amount, compared with the reduction in DGDG.

The decrease in MGDG during L-CO_2 acclimation correlates with the high level of expression of the TAG-lipase-encoding gene *PGD1* in L-CO_2 cells (Fig. 5) and with the evidence provided by Legeret et al. [42] that in stressed *C. reinhardtii* cells MGDGs are converted into storage lipids (TAG) via DAG intermediates. Further support for this suggestion is given by Legeret et al. [42] who also observed that the level of membrane lipids decreased and the TAG level increased, while the total cellular fatty acid content did not vary, under heat-stress conditions. In agreement with the above, the total lipids in our L-CO_2 cells did not differ significantly from those of H-CO_2 cells (Fig. S3), indicating that membrane lipids were not degraded but rather converted to storage lipids. The fact that some TAGs in LDF contain C_{16} in the *sn2* of the glycerol backbone points to the plastid reassembly of these TAGs.

Since stressogenic conditions cause an increase in LDs and the lipid monolayer of LDs contains mainly DGTS [18,59,60], it is not surprising that DGTS showed the most pronounced increase of all the glycerolipids during CCM induction (Figs. 1 and 2, Table S3). We did not detect any differences in expression of *BTA1*, the gene encoding the enzyme diacylglyceryl-*N*,*N*,*N*-trimethylhomoserine synthesis protein (BTA1) which is involved in DGTS biosynthesis in *C. reinhardtii* [15,26]. The lack of *BTA1* upregulation may be because its regulation is at the post-translational level. Among the DGTS species, of which the level significantly increased in L-CO_2 cells, we found DGTS 32:0, containing C_{16} in the glycerol *sn2* position. This means that it originated not from the ER, as is typical for DGTS synthesis [30], but reassembled in the chloroplast as for TAG; this has not previously been reported for *C. reinhardtii*.

Under L-CO_2 we observed the induction of *MLDP1* transcription. *MLDP1* encodes the major lipid droplet protein (MLDP), which is an important structural component of the surface of *C. reinhardtii* LDs [18]. Moreover, transcription of *BCX1*, a gene encoding a β-subunit of the acetyl-CoA carboxylase that converts acetylCoA to malonylCoA, was upregulated under L-CO_2 (Fig. 5C). MalonylCoA can be converted to malonyl ACP and further to other acyl-ACPs such as palmitoyl-ACP or steroyl-ACP. Acyl-ACPs can be directly hydrolyzed into free fatty acids by the enzyme FAT1 or diverted to phosphatidic acid (PA) and then directed to DAG biosynthesis. Although we observed decreased expression of genes encoding enzymes of phospholipid biosynthesis, including *KDG1* (diacylglycerol kinase), *INO1* (inositol-3-phosphate synthase) and *SDC1* (serine decarboxylase – phosphatidylethanolamine), the increased expression of *FAT1*suggests that, during the induction of the CCM, the carbon flow was diverted in the direction of free fatty acids and then, transferred to DAG via LCL1 for subsequently TAG biosynthesis (Fig. 6). The above is consistent with bioenergetics analyses indicating that *C. reinhardtii* prefers to maximize lipid production when it is difficult to generate new cells, e.g. under nutrient limitation [61].

One known effect of stressogenic factors on *C. reinhardtii* metabolism is the co-occurrence of lipid remodeling and carotenoid biosynthesis [12]. Our analysis of the LD fraction revealed ketocarotenoids, xanthophylls and carotenes common in LDF (astaxanthin, β-carotene), but also species that are typically present in the chloroplast. Only astaxanthin and β-carotene have previously been detected in *H. pluvialis* LDs [34,62]. However, *C. reinhardtii* cells contain two different classes of LDs: cytoplasmic and plastidial [63]. The cytoplasmic LDs tend to accumulate greater amounts of neutral lipids and they are usually larger than plastidial LDs (plastoglobules), which are probably involved in stress responses, especially in protecting membranes from photooxidation and protecting photosystem II from photoinactivation [16,64]. Disruption of microalgal cells during the LDF isolation usually damages both the plasmalemma and envelope membranes, making it almost impossible to separate the different LDs classes and rendering contamination of the LD fraction with cytoplasmic, plastidial and mitochondrial lipids highly probable [15,26]. The methodology used for LDF isolation in the present study did not allow us to avoid such a possibility.

The transcript analysis performed in this work also revealed changes in the transcription of genes related to carotenoid biosynthesis during the CCM induction. Transcription of *CYP97A6*, encoding a carotenoid hydroxylase involved in zeaxanthin production [65], was highly upregulated throughout the L-CO_2 treatment. The enhanced synthesis of zeaxanthin is common in cells subjected to perturbations such as the transient CO_2 limitation we applied: zeaxanthin is one of the key antioxidants in the chloroplast membranes and a major component in the deactivation of excited singlet chlorophyll (^{1}Chl*) [66]. Zeaxanthin is generated in the xanthophyll cycle from violaxanthin via antheraxanthin; it typically accumulates when electron transport is oversaturated. In our dataset, both zeaxanthin and violaxanthin increased during L-CO_2 acclimation (Figs. 3, 6) indicating low efficiency of the violaxanthin – zeaxanthin interconversion. This seems to be supported by the low abundance of the transcript of violaxanthin de-epoxidase (*VDR1*) (Fig. 6). Inefficient violaxanthin de-epoxidation could be connected with the low level of MGDG noted in L-CO_2 cells, since loss of MGDG results in higher conductivity of the thylakoid and an increase in luminal pH, causing the activity of violaxanthin de-epoxidase decrease [56]. MGDG is also necessary to release violaxanthin from the membrane and make it available for violaxanthin de-epoxidase [67]. In addition to its role in the energy dissipation in the xanthophyll cycle, violaxanthin is thought to be a protector of antenna pigments; zeaxanthin is involved in the thylakoid lipid protection under photo-inhibitory condition [20]. Thus, the balance violaxanthin/zeaxanthin is an important element of cellular acclimation to environmental perturbations.

Another stress-induced carotenoid [34] accumulated in L-CO_2 cells was astaxanthin (Fig. 6) which is believed to be the end-product of a multicomponent protection processes [68]. It has been shown that the reducing power (as NADPH) required for the synthesis of TAGs and fatty acid molecules needed for astaxanthin esterification serves as an electron sink under photo-oxidative stress [68]. Our data showed the presence of both free and esterified species of ketocarotenoids in the LDF. Furthermore, the biosynthesis of astaxanthin has been shown to diminish ROS production by lowering the cellular oxygen concentration due to the formation of oxygen-rich molecules and by channeling electron transport from the carotenogenic desaturation steps to the plastoquinones and then to the plastidial terminal oxidase (PTOX) [69]. Wang et al. [14] have shown that in *Haematococcus pluvialis* the transcription of *PTOX1* was positively correlated with astaxanthin accumulation. In contrast, we observed upregulation of *PTOX2* under L-CO_2 conditions. In *C. reinhardtii* PTOX1 is involved in the regeneration of oxidized plastoquinone for phytoene desaturation, while PTOX2 operates in chlororespiration and protects cells from light stress [70]. It therefore seems that, during CCM induction, PTOX2-mediated chlororespiration is a component of the stress response system preventing over-reduction of the electron transfer chain, as has been described for responses to high/low temperature, water deficiency and high

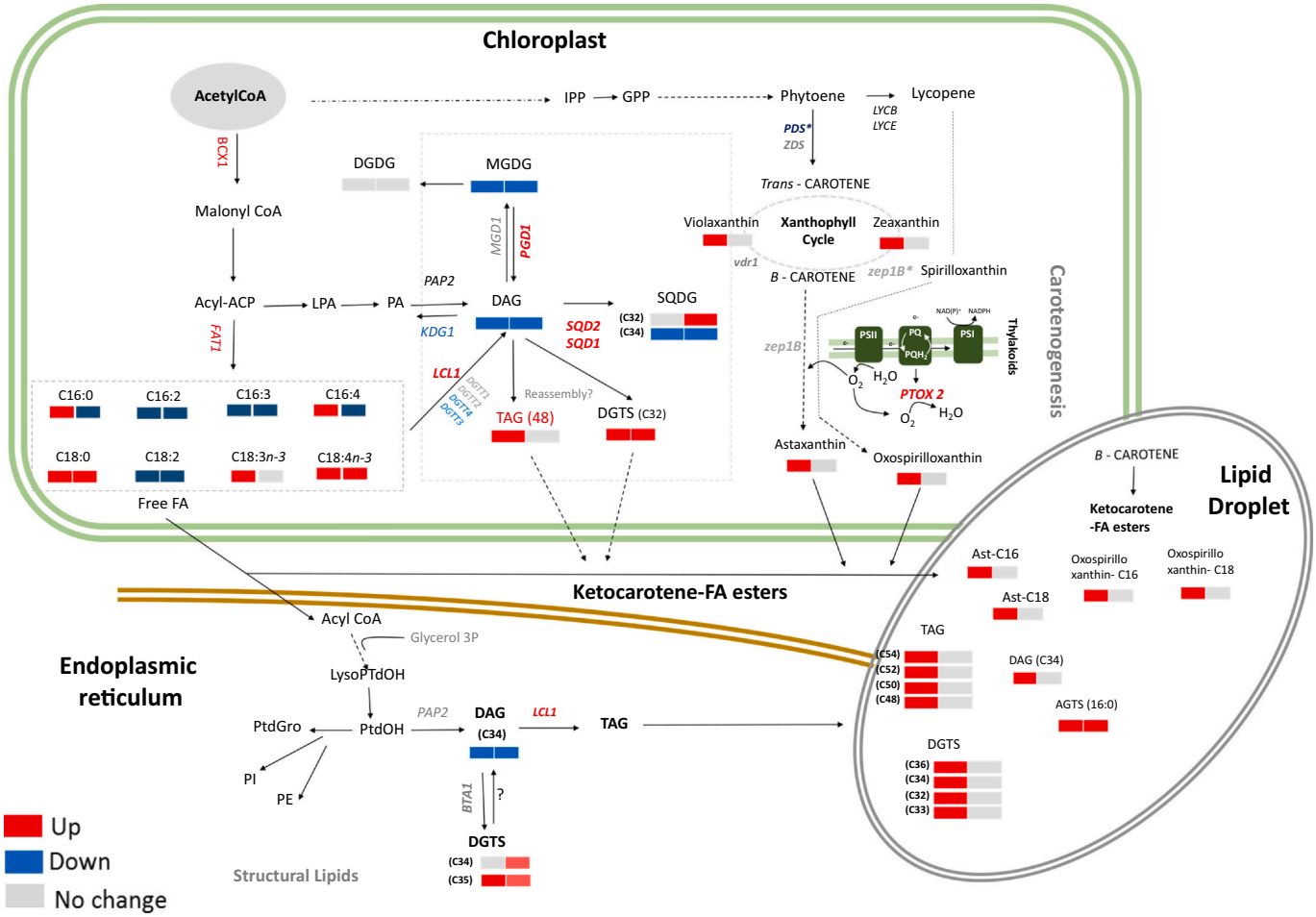

Fig. 6. Model of lipid metabolism changes in *Chlamydomonas reinhardtii* under limiting CO_2 conditions.

irradiance [71].

In conclusion, the results presented here also support our previous work [6] where we proposed a model in which CCM is the result of "several relatively small but orchestrated changes in metabolite profiles". Here, the model is enhanced with lipidomic and transcript data, enabling us to suggest that some of these metabolic changes, including lipid remodeling and carotenoid biosynthesis, are directed towards reducing the effects of oxidative stress caused by transient CO_2 shortage. Thus, CCM establishment seems to consist of two parallel processes. The first, which includes stimulation of carbonic anhydrases, CO_2/HCO_3^- transporters etc., prepares the cell for living in a low-CO_2 environment. The second, which involves photorespiration, chlororespiration, lipid remodeling and carotenoid synthesis/conversion, enables the cell to survive the oxidative stress until its CCM reaches maximum efficiency.

Supplementary data to this article can be found online at https://doi.org/10.1016/j.algal.2020.102099.

Funding information

This work was supported by Knut and Alice Wallenberg Foundation, Sweden [grant number KAW 2011.02.12 to T.M.], and corresponding co-funding from Swedish University of Agricultural Sciences to T.M. This work was also supported by Bio4Energy (Swedish Programme for Renewable Energy), VINNOVA (the Swedish Governmental Agency for Innovation Systems) and KAW (The Knut and Alice Wallenberg Foundation). A.K.B. Would like thank Carl Tryggers, Sven and Lilly Lawski's Foundation, Sweden, for Postdoctoral fellowship.

Statement regarding informed consent, human/animal rights

No conflicts, informed consent, human or animal rights applicable for this work.

CRediT authorship contribution statement

Ilka N. Abreu: conceptualization, methodology, investigation, formal analysis, visualization, writing- reviewing and editing; Anna Aksmann: conceptualization, methodology, investigation, formal analysis, writing- reviewing and editing; Amit K. Bajhaiya: investigation; Reyes Benlloch: Maurio Giordani: conceptualization, writing- reviewing and editing; investigation; Wojciech Pokora: investigation; Eva Selstam: investigation, writing- reviewing and editing; Thomas Moritz: conceptualization, methodology, writing- reviewing and editing, supervision.

Declaration of competing interest

The authors declare that they have no known competing financial interests or personal relationships that could have appeared to influence the work reported in this paper.

Acknowledgement

We would like to thank Prof. Göran Samuelsson for encouraging discussions in planning of the experiments. Swedish Metabolomics Centre is acknowledged for technical support.

References

[1] J.A. Raven, J. Beardall, M. Giordano, Energy costs of carbon dioxide concentrating mechanisms in aquatic organisms, Photosynth. Res. 121 (2–3) (2014) 111–124.
[2] M. Giordano, J. Beardall, J.A. Raven, CO_2 concentrating mechanisms in algae: mechanisms, environmental modulation, and evolution, Annu. Rev. Plant Biol. 56 (2005) 99–131.
[3] J.A. Raven, M. Giordano, J. Beardall, S.C. Maberly, Algal and aquatic plant carbon concentrating mechanisms in relation to environmental change, Photosynth. Res. 109 (1–3) (2011) 281–296.
[4] J.V. Moroney, N. Jungnick, R.J. DiMario, D.J. Longstreth, Photorespiration and carbon concentrating mechanisms: two adaptations to high O_2, low CO_2 conditions, Photosynth. Res. 117 (1–3) (2013) 121–131.
[5] J.A. Raven, Inorganic carbon acquisition by eukaryotic algae: four current questions, Photosynth. Res. 106 (1–2) (2010) 123–134.
[6] L. Renberg, A.I. Johansson, T. Shutova, H. Stenlund, A. Aksmann, J.A. Raven, P. Gardestrom, T. Moritz, G. Samuelsson, A Metabolomic approach to study major metabolite changes during acclimation to limiting CO_2 in Chlamydomonas reinhardtii, Plant Physiol. 154 (2010) 187–196.
[7] A. Vardi, I. Berman-Frank, T. Rozenberg, O. Hadas, A. Kaplan, A. Levine, Programmed cell death of the dinoflagellate Peridinium gatunense is mediated by CO_2 limitation and oxidative stress, Curr. Biol. 9 (18) (1999) 1061–1064.
[8] S.C. Burey, V. Poroyko, Z.N. Ergen, S. Fathi-Nejad, C. Schuller, N. Ohnishi, H. Fukuzawa, H.J. Bohnert, W. Loffelhardt, Acclimation to low CO_2 by an inorganic carbon-concentrating mechanism in Cyanophora paradoxa, Plant Cell Environ. 30 (2007) 1422–1435.
[9] J. Fan, H. Xu, Y. Luo, M. Wan, J. Huang, W. Wang, Y. Li, Impacts of CO_2 concentration on growth, lipid accumulation, and carbon-concentrating-mechanism-related gene expression in oleaginous Chlorella, Appl. Microbiol. Biotechnol. 99 (5) (2015) 2451–2462.
[10] C.S. Im, Z.D. Zhang, J. Shrager, C.W. Chang, A.R. Grossman, Analysis of light and CO_2 regulation in Chlamydomonas reinhardtii using genome-wide approaches, Photosynth. Res. 75 (2003) 111–125.
[11] L.D. Roberts, G. McCombie, C.M. Titman, J.L. Griffin, A matter of fat: an introduction to lipidomic profiling methods, J. Chromatogr. B 871 (2) (2008) 174–181.
[12] A.K. Minhas, P. Hodgson, C.J. Barrow, A. Adholeya, A review on the assessment of stress conditions for simultaneous production of microalgal lipids and carotenoids, Front. Microbiol. 7 (2016) 546.
[13] M. Siaut, S. Cuiné, C. Cagnon, B. Fessler, M. Nguyen, P. Carrier, A. Beyly, F. Beisson, C. Triantaphylidès, Y.L. Beisson, G. Peltier, Oil accumulation in the model green alga Chlamydomonas reinhardtii: characterization, variability between common laboratory strains and relationship with starch reserves, BMC Biotechnol. 11 (1) (2011) 7.
[14] J.X. Wang, M. Sommerfeld, Q. Hu, Occurrence and environmental stress responses of two plastid terminal oxidases in Haematococcus pluvialis (Chlorophyceae), Planta 230 (2009) 191–203.
[15] H.M. Nguyen, M. Baudet, S. Cuine, J.M. Adriano, D. Barthe, E. Billon, C. Bruley, F. Beisson, G. Peltier, M. Ferro, Y. Li-Beisson, Proteomic profiling of oil bodies isolated from the unicellular green microalga Chlamydomonas reinhardtii: with focus on proteins involved in lipid metabolism, Proteomics 11 (2011) 4266–4273.
[16] C. Bréhélin, F. Kessler, K.J. van Wijk, Plastoglobules: versatile lipoprotein particles in plastids, Trends Plant Sci. 12 (6) (2007) 260–266.
[17] T. Fujimoto, Y. Ohsaki, J. Cheng, M. Suzuki, Y. Shinohara, Lipid droplets: a classic organelle with new outfits, Histochem. Cell Biol. 130 (2) (2008) 263–279.
[18] B.S. Liu, C. Benning, Lipid metabolism in microalgae distinguishes itself, Curr. Opin. Biotechnol. 24 (2013) 300–309.
[19] S. Ota, A. Morita, S. Ohnuki, A. Hirata, S. Sekida, K. Okuda, Y. Ohya, S.J. Kawano, Carotenoid dynamics and lipid droplet containing astaxanthin in response to light in the green alga Haematococcus pluvialis, Sci. Rep. 8 (2018) 5617.
[20] W.I. Gruszecki, K. Strzałka, Carotenoids as modulators of lipid membrane physical properties, Biochim. Biophys. Acta (BBA)-Molecular Basis of Disease 1740 (2) (2005) 108–115.
[21] A. Izumo, S. Fujiwara, Y. Oyama, A. Satoh, N. Fujita, Y. Nakamura, M. Tsuzuki, Physicochemical properties of starch in Chlorella change depending on the CO_2 concentration during growth: comparison of structure and properties of pyrenoid and stroma starch, Plant Sci. 172 (6) (2007) 1138–1147.
[22] N. Sato, M. Tsuzuki, A. Kawaguchi, Glycerolipid synthesis in Chlorella kessleri 11 h: II. Effect of the CO_2 concentration during growth, Biochim. Biophys. Acta (BBA)-Molecular and Cell Biology of Lipids 1633 (1) (2003) 35–42.
[23] N. Sueoka, Mitotic replication of deoxyribonucleic acid in Chlamydomonas reinhardi, Proc. Natl. Acad. Sci. 46 (1) (1960) 83–91.
[24] R.A. Andersen (Ed.), Algal Culturing Techniques, Elsevier Academic Press, 2005.
[25] C. Bolling, O. Fiehn, Metabolite profiling of Chlamydomonas reinhardtii under nutrient deprivation, Plant Physiol. 139 (2005) 1995–2005.
[26] E.R. Moellering, C. Benning, RNA interference silencing of a major lipid droplet protein affects lipid droplet size in Chlamydomonas reinhardtii, Eukaryot. Cell 9 (1) (2010) 97–106.
[27] A.J. Ytterberg, J.B. Peltier, K.J. van Wijk, Protein profiling of plastoglobules in chloroplasts and chromoplasts. A surprising site for differential accumulation of metabolic enzymes, Plant Physiol. 140 (2006) 984–997.
[28] E.G. Bligh, W.J. Dyer, A rapid method of total lipid extraction and purification, Can. J. Biochem. Physiol. 37 (8) (1959) 911–917.
[29] N. Schauer, D. Steinhauser, S. Strelkov, D. Schomburg, G. Allison, T. Moritz, K. Lundgren, U.R. Tunali, M.G. Forbes, L. Willmitzer, A.R. Fernie, J. Kopka, GC–MS libraries for the rapid identification of metabolites in complex biological samples, FEBS Lett. 579 (6) (2005) 1332–1337.
[30] Y. Li-Beisson, F. Beisso, W. Riekhof, Metabolism of acyl-lipids in Chlamydomonas reinhardtii, The Plant J. 82 (2015) 504–522.
[31] R. Miller, G. Wu, R.R. Deshpande, A. Vieler, K. Gärtner, X. Li, E.R. Moellering, S. Zäuner, A.J. Cornish, B. Liu, B. Bullard, B.B. Sears, M.H. Kuo, E.L. Hegg, Y.S. Hill, S.H. Shiu, C. Benning, Changes in transcript abundance in Chlamydomonas reinhardtii following nitrogen deprivation predict diversion of metabolism, Plant Physiol. 154 (2010) 1737–1752.
[32] E.I. Urzica, A. Vieler, A. Hong-Hermesdorf, M.D. Page, D. Casero, S.D. Gallaher, J. Kropat, M. Pellegrini, C. Benning, S.S. Merchant, Remodeling of membrane lipids in iron starved Chlamydomonas, J. Biol. Chem. 288 (2013) 30246–30258, https://doi.org/10.1074/jbc.M113.490425.
[33] C.I. Cazzonelli, B.J. Pogson, Source to sink: regulation of carotenoid biosynthesis in plants, Trends Plant Sci. 15 (2010) 266–274.
[34] A.E. Solovchenko, Recent breakthroughs in the biology of astaxanthin accumulation by microalgal cell, Photosynth. Res. 125 (2015) 437–449.
[35] A.J. Brueggeman, D.S. Gangadharaiah, M.F. Cserhati, D. Casero, D.P. Weeks, I. Ladunga, Activation of the carbon concentrating mechanism by CO_2 deprivation coincides with massive transcriptional restructuring in Chlamydomonas reinhardtii, Plant Cell 24 (2012) 1860–1875.
[36] K Miura, T Yamano, S Yoshioka, T Kohinata, Y Inoue, F Taniguchi, ... K Ohyama, Expression profiling-based identification of CO2-responsive genes regulated by CCM1 controlling a carbon-concentrating mechanism in Chlamydomonas reinhardtii, Plant physiology 135 (3) (2004) 1595–1607.
[37] R.A. Ynalvez, Y. Xiao, A.S. Ward, K. Cunnusamy, J.V. Moroney, Identification and characterization of two closely related β-carbonic anhydrases from Chlamydomonas reinhardtii, Physiol. Plant. 133 (1) (2008) 15–26.
[38] S. Yoshioka, F. Taniguchi, K. Miura, T. Inoue, T. Yamano, H. Fukuzawa, The novel Myb transcription factor LCR1 regulates the CO2-responsive gene Cah1, encoding a periplasmic carbonic anhydrase in Chlamydomonas reinhardtii, Plant Cell 16 (6) (2004) 1466–1477.
[39] N. Atkinson, D. Feike, L. Mackinder, M.T. Meyer, H. Griffiths, M.C. Jonikas, A.M. Smith, A.J. McCormick, Introducing an algal carbon-concentrating mechanism into higher plants: location and incorporation of key components, Plant Biotechnol. J. 14 (2016) 1302–1315.
[40] X. Li, E.R. Moellering, B. Liu, A Galactoglycerolipid lipase is required for triacylglycerol accumulation and survival following nitrogen deprivation in Chlamydomonas reinhardtii, Plant Cell 24 (2012) 4670–4686.
[41] G. Chen, B. Wang, D. Han, M. Sommerfeld, Y. Lu, F. Chen, Q. Hu, Molecular mechanisms of the coordination between astaxanthin and fatty acid biosynthesis in Haematococcus pluvialis (Chlorophyceae), The Plant J. 81 (2015) 95–107.
[42] B. Legeret, M. Schulz-Raffelt, H.M. Nguyen, P. Auroy, F. Beisson, G. Peltier, G. Blanc, Y. Li-Beisson, Lipidomic and transcriptomic analyses of Chlamydomonas reinhardtii under heat stress unveil a direct route for the conversion of membrane lipids into storage lipids, Plant Cell Environ. 39 (2016) 834–847.
[43] I. Polukhina, R. Fristedt, E. Dinc, P. Cardol, R. Croce, Carbon supply and photoacclimation cross talk in the green alga Chlamydomonas reinhardtii, Plant Physiol. 172 (3) (2016) 1494–1505.
[44] F.V. Winck, D.O.P. Melo, A.F.G. Barrios, Carbon acquisition and accumulation in microalgae Chlamydomonas: insights from "omics" approaches, J. Proteome 94 (2013) 207–218.
[45] T. Ott, J. Clarke, K. Birks, G. Johnson, Regulation of the photosynthetic electron transport chain, Planta 209 (2) (1999) 250–258.
[46] K. Asada, Radical production and scavenging in the chloroplasts, Photosynthesis and the Environment, Springer, Dordrecht, 1996, pp. 123–150.
[47] M.J. Fryer, J.R. Andrews, K. Oxborough, D.A. Blowers, N.R. Baker, Relationship between CO_2 assimilation, photosynthetic electron transport, and active O_2 metabolism in leaves of maize in the field during periods of low temperature, Plant Physiol. 116 (2) (1998) 571–580.
[48] T. Karuppanapandian, J.C. Moon, C. Kim, K. Manoharan, W. Kim, Reactive oxygen species in plants: their generation, signal transduction, and scavenging mechanisms, Australian J. Crop Sci. 5 (6) (2011) 709.
[49] P. Sharma, A.B. Jha, R.S. Dubey, M. Pessarakli, Reactive oxygen species, oxidative damage, and antioxidative defense mechanism in plants under stressful conditions, J. Bot. 2012 (2012) 217037, https://doi.org/10.1155/2012/217037.
[50] C. Pan, G.J. Ahammed, X. Li, K. Shi, Elevated CO_2 improves photosynthesis under high temperature by attenuating the functional limitations to energy fluxes, electron transport and redox homeostasis in tomato leaves, Front. Plant Sci. 9 (2018) 1739.
[51] K. Suzuki, H. Uchida, T.G. Mamedov, The phosphoglycolate phosphatase gene and the mutation in the phosphoglycolate phosphatase-deficient mutant (pgp1-1) of Chlamydomonas reinhardtii, Can. J. Bot. 83 (2005) 842–849.
[52] A.K. Hurlock, R.L. Roston, K. Wang, C. Benning, Lipid trafficking in plant cells, Traffic 15 (9) (2014) 915–932.
[53] Z.Y. Du, B.F. Lucker, K. Zienkiewicz, T.E. Miller, A. Zienkiewicz, B.B. Sears, D. Kramer, C. Benning, Galactoglycerolipid lipase PGD1 is involved in thylakoid membrane remodeling in response to adverse environmental conditions in Chlamydomonas, Plant Cell 30 (2018) 447–465, https://doi.org/10.1105/tpc.17.00446.
[54] L. Boudière, M. Michaud, D. Petroutsos, F. Rébeillé, D. Falconet, O. Bastien, M.A. Block, E. Maréchal, Glycerolipids in photosynthesis: composition, synthesis and trafficking, Biochim. Biophys. Acta (BBA)-Bioenergetics 1837 (4) (2014) 470–480.
[55] B. De Kruijff, Lipids beyond the bilayer, Nature 386 (6621) (1997) 129.
[56] H. Aronsson, M.A. Schöttler, A.A. Kelly, C. Sundqvist, P. Dörmann, S. Karim,

P. Jarvis, Mongalactosyldiacylglycerol deficiency in Arabidopsis affects pigment composition in the prolamellar body and impairs thylakoid membrane ernergization and photoprotection, Plant Physiol. 148 (2008) 580–592.
[57] S. Fujii, K. Kobayashi, Y. Nakamura, H. Wada, Inducible knockdown of mongalactosyldiacylglycerol synthase1 reveals roles of galactolipids in organelle differentiation in Arabidopsis cotyledons, Plant Physiol. 166 (2014) (1436-144).
[58] L. Xiaoxiao, M. Dengke, Z. Zhiyong, W. Shiwen, Sheng, D. Xiping, Y. Lina, Plant lipid remodeling in response to abiotic stresses, Environ. Exp. Bot. 165 (2019) 174–184.
[59] K. Grünewald, J. Hirschberg, C. Hagen, Ketocarotenoid biosynthesis outside of plastids in the unicellular green alga Haematococcus pluvialis, J. Biol. Chem. 276 (8) (2001) 6023–6029.
[60] C. Tsai, K. Zienkiewicz, C.L. Amstutz, B.G. Brink, J. Warakanont, R. Roston, C. Benning, Dynamics of protein and polar lipid recruitment during lipid droplet assembly in Chlamydomonas reinhardtii, The Plant J. 83 (2015) 650–660.
[61] K. Küçük, R. Tevatia, E. Sorgüven, Y. Demirel, M. Özilgen, Bioenergetics of growth and lipid production in Chlamydomonas reinhardtii, Energy 83 (2015) 503–510.
[62] A.M. Collins, M. Aaron, H.D.T. Jones, D.X. Han, Q. Hu, T.E. Beechem, J.A. Timlin, Carotenoid distribution in living cells of Haematococcus pluvialis (Chlorophyceae), PLoS One 6 (2011) e24302.
[63] H. Goold, F. Beisson, G. Peltier, Y. Li-Beisson, Microalgal lipid droplets: composition, diversity, biogenesis and functions, Plant Cell Rep. 34 (4) (2015) 545–555.
[64] L. Davidi, E. Shimoni, I. Khozin-Goldberg, A. Zamir, U. Pick, Origin of b-carotene-rich plastoglobuli in Dunaliella bardawi, Plant Physiol. 164 (2014) 2139–2156.
[65] B. Schoefs, N.E. Rmiki, J. Rachadi, Y. Lemoine, Astaxanthin accumulation in *Haematococcus* requires a cytochrome P450 hydroxylase and an active synthesis of fatty acids, FEBS Lett. 3 (2001) 125–128.
[66] P. Jahns, A.R. Holzwarth, The role of the xanthophyll cycle and of lutein in photoprotection of photosystem II, Biochim. Biophys. Acta (BBA)-Bioenergetics 1817 (1) (2012) 182–193.
[67] S. Schaller, D. Latowski, M. Jemioła-Rzemińska, C. Wilhelm, K. Strzałka, R. Goss, The main thylakoid membrane lipid monogalactosyldiacylglycerol (MGDG) promotes the de-epoxidation of violaxanthin associated with the light-harvesting complex of photosystem II (LHCII), Biochim. Biophys. Acta (BBA)-Bioenergetics 1797 (3) (2010) 414–424.
[68] Y. Lemoine, B. Schoefs, Secondary ketocarotenoid astaxanthin biosynthesis in algae: a multifunctional response to stress, Photosynth. Res. 106 (1–2) (2010) 155–177.
[69] Y. Li, M. Sommerfeld, F. Chen, Q. Hu, Consumption of oxygen by astaxanthin biosynthesis: a protective mechanism against oxidative stress in Haematococcus pluvialis (Chlorophyceae), J. Plant Physiol. 165 (17) (2008) 1783–1797.
[70] L. Houille-Vernes, F. Rappaport, F.A. Wollman, J. Alric, X. Johnson, Plastid terminal oxidase 2 (PTOX2) is the major oxidase involved in chlororespiration in Chlamydomonas, Proc. Nat. Academy Sci. 108 (51) (2011) 20820–20825.
[71] D. Rumeau, G. Peltier, L. Cournac, Chlororespiration and cyclic electron flow around PSI during photosynthesis and plant stress response, Plant Cell Environ. 30 (9) (2007) 1041–1051.